Hindawi
International Journal of Photoenergy
Volume 2018, Article ID 2140797, 9 pages
https://doi.org/10.1155/2018/2140797

Research Article

Grid-Connected Photovoltaic System with Active Power Filtering Functionality

Joaquín Vaquero,[1] **Nimrod Vázquez**,[2] **Ivan Soriano**,[1] **and Jeziel Vázquez**[3]

[1]*Electronics Technology Area, Rey Juan Carlos University, 28933 Mostoles, Madrid, Spain*
[2]*Electronics Engineering Department, Technological Institute of Celaya, 38010 Celaya, GTO, Mexico*
[3]*Computer Engineering Department, Superior Technological Institute of South of Guanajuato, 38980 Uriangato, GTO, Mexico*

Correspondence should be addressed to Nimrod Vázquez; n.vazquez@ieee.org

Received 2 December 2017; Accepted 3 April 2018; Published 2 May 2018

Academic Editor: Jegadesan Subbiah

Solar panels are an attractive and growing source of renewable energy in commercial and residential applications. Its use connected to the grid by means of a power converter results in a grid-connected photovoltaic system. In order to optimize this system, it is interesting to integrate several functionalities into the power converter, such as active power filtering and power factor correction. Nonlinear loads connected to the grid generate current harmonics, which deteriorates the mains power quality. Active power filters can compensate these current harmonics. A photovoltaic system with added harmonic compensation and power factor correction capabilities is proposed in this paper. A sliding mode controller is employed to control the power converter, implemented on the CompactRIO digital platform from National Instruments Corporation, allowing user friendly operation and easy tuning. The power system consists of two stages, a DC/DC boost converter and a single-phase inverter, and it is able to inject active power into the grid while compensating the current harmonics generated by nonlinear loads at the point of common coupling. The operation, design, simulation, and experimental results for the proposed system are discussed.

1. Introduction

Nowadays, with the increasing energy demand and its price increment, along with the scarcity of nonrenewable resources such as oil, natural gas, and coal, researchers are looking for new energy sources to meet the current energy needs. This has led to innovative solutions with desirable characteristics, such as greater efficiency, more power, and less pollution when generating energy [1].

An important issue is power quality, which is influenced by the growing use of nonlinear loads by residential, commercial, and industrial consumers. This type of load generates high harmonic currents that interact with the grid impedance, causing harmonic voltages which affect all users connected to the same point of common coupling (PCC).

Among the problems caused by the presence of harmonics are distortion of the AC mains voltage within the facilities, high currents flowing through the neutral conductor, overheating of transformers and conductors, poor operation of switches and fuses, erroneous operation of electronic equipment, life reduction in incandescent lamps, resonance risk in fluorescent lamps, and overheating of rotating machines [2]. Active power filters have been proposed to compensate the current harmonics [3–5]. Although they provide a good compensation system, their high cost is a considerable disadvantage.

The growth of distributed generation (DG) has been favored by the use of renewable energies. The main power conversion stage in a DG system is the inverter, which is very flexible from a control point of view. This flexibility allows exploration of the possibility of injecting active power to the grid from a photovoltaic (PV) system while compensating current harmonics.

Some papers have proposed the use of multifunctional inverters [6–9]. Researchers in [6] proposed the use of resonant tanks which are capable of effectively removing selected harmonics, but many resonant tanks are needed to remove the number of harmonics. Instantaneous reactive power

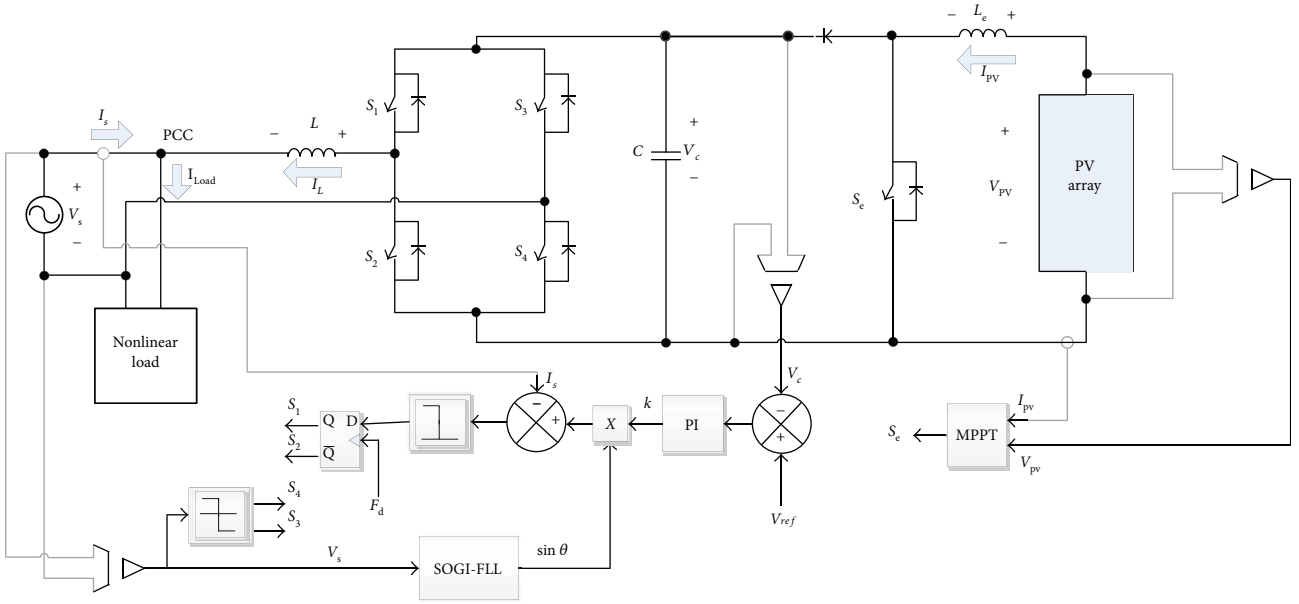

Figure 1: Block diagram of the power stage with a sliding mode controller.

theory has also been used in [7–9]. However, this is only applicable to three-phase systems. In [9], the synchronous reference frame theory is used, usually applied to three-phase systems, but it requires virtual signals when used in single-phase systems.

In this paper, a PV system with active power filtering functionality and a controller based on sliding mode is analyzed, implemented, and tested. The authors have previously presented the simulation results of this proposal in [10], adding now experimental results, discussion on implementation issues, and a complete design and analysis of the system, which corroborates the conclusions of the previous work. The system consists of a single-phase two-stage converter (Figure 1). This converter is able to inject both active and reactive power and, additionally, to compensate the harmonic currents at the PCC. The sliding mode control brings the advantage of easy implementation with few computational resources compared to other techniques discussed above. In addition, it does not need an independent control loop as in [6] to generate the reference signal.

The paper is organized as follows: the power stage, the controller, and implementation are described, the simulation and experimental results are then illustrated, and finally, the conclusions are given.

2. Work Bench and Multifunctional System

The power stage consists of a DC/DC boost converter, an energy storage capacitor, a full-bridge single-phase inverter, and an output inductor connected to the grid (Figure 1). The switching devices used are a new generation of silicon carbide (SiC) metal-oxide-semiconductor field-effect transistor (MOSFET). The digital platform for the controller implementation is the CompactRIO from National Instruments Corporation (NI), together with LabVIEW software, which allows a flexible visual programming environment.

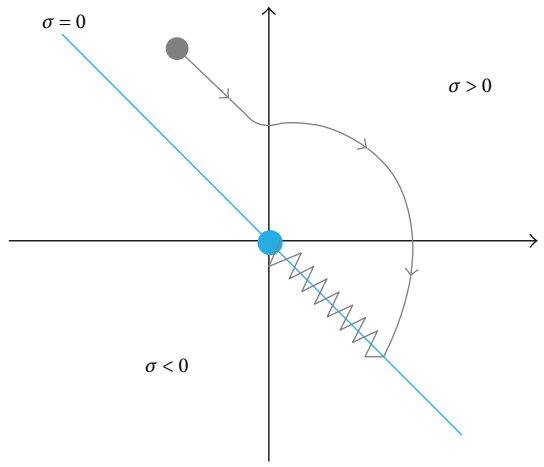

Figure 2: Evolution of the system with a sliding mode controller.

The DC/DC boost converter demands the available power from the PV panels by means of a maximum power point tracking algorithm (MPPT). The inverter injects active power generated by the PV panels to the grid and compensates the current harmonic content at the PCC. The entire control tasks for both converters have been implemented in the NI platform.

2.1. The Power Stage. In order to simplify the analysis of the power stage, the PV panels and the DC/DC boost converter can be considered to behave as a current source, since changes in the energy provided by the PV panels take longer than the AC mains period.

The converter is operated to produce a unipolar output voltage. Each branch of the inverter is switched independently, with S_3 and S_4 activated every half-period of the AC mains and S_1 and S_2 activated following a pulse width

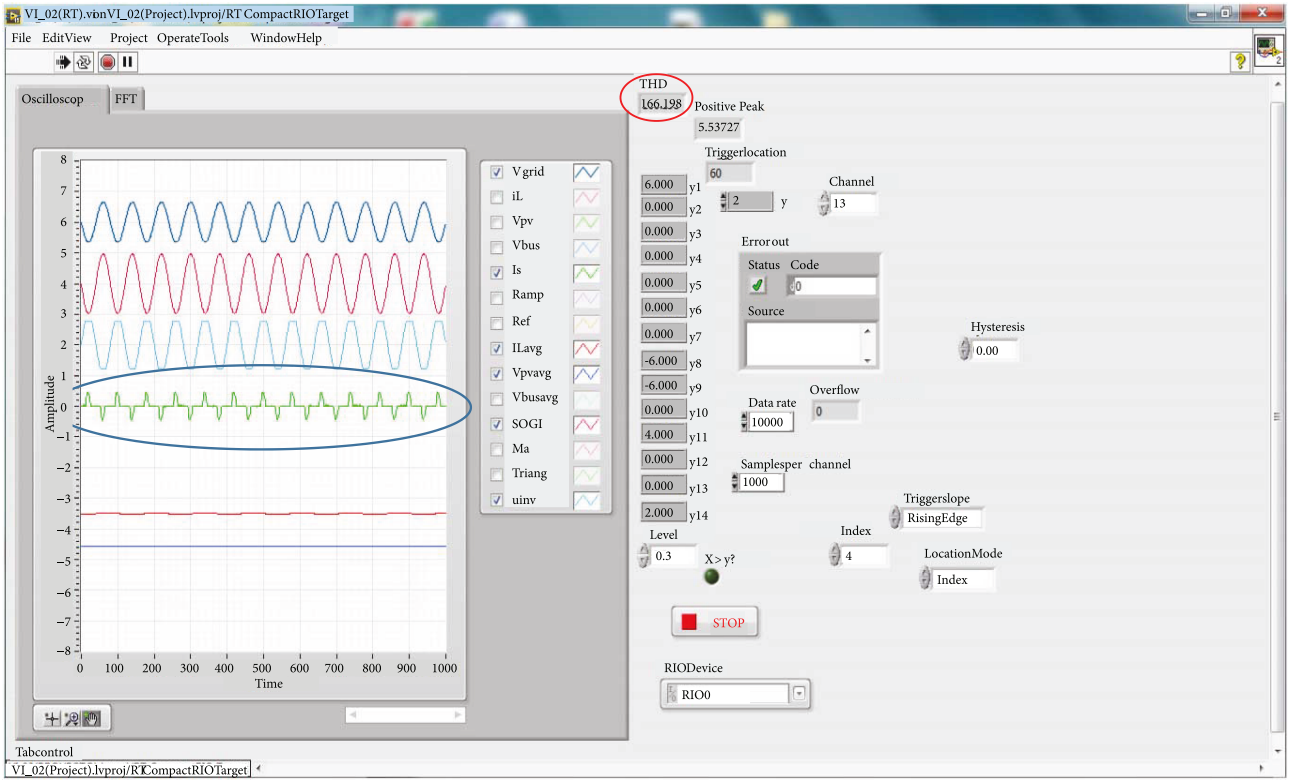

Figure 3: Implemented LabVIEW control panel.

modulation (PWM) pattern, in order to control the injected current to the grid.

2.1.1. Modelling the Power Stage. Considering the above simplification, the model of the system is

$$\begin{aligned}\frac{di_L}{dt} &= \frac{v_c}{L}(u_1 - u_3) - \frac{v_s}{L},\\ \frac{dv_c}{dt} &= -\frac{i_L}{C}(u_1 - u_3) + \frac{i_{PV}}{C},\end{aligned} \tag{1}$$

where i_L is the inductor current, v_c is the capacitor voltage, i_{PV} represents the energy provided by the PV panels and the boost converter, u_x is the control signal for switch S_x (1 = on, 0 = off), and v_s is the AC mains voltage.

The switches of the same branch are complementary; hence,

$$\begin{aligned}u_1 + u_2 &= 1,\\ u_3 + u_4 &= 1.\end{aligned} \tag{2}$$

For a model of the PV panel, see that proposed in [11].

2.2. Design of the Power Stage. The capacitor is calculated considering the stored energy and the low-frequency component of the capacitor voltage ripple. The following equation is first used:

$$\Delta E = \frac{1}{2}C\left(v_{cf}^2 - v_{co}^2\right), \tag{3}$$

where ΔE is the energy stored in the capacitor and v_{cf} and v_{co} are the capacitor voltages due to the ripple.

The low frequency of the capacitor voltage ripple is twice the grid frequency. Considering that the stored energy handled by the system in each half of the AC mains period is 10% of the nominal output energy and that the capacitor voltages due to the ripple are $v_{cf} = (v_c + \Delta v_c)/2$ and $v_{co} = (v_c - \Delta v_c)/2$, (4) is obtained:

$$C = \frac{0.1\,P}{2v_c\Delta v_c f_o}, \tag{4}$$

where Δv_c is the desired ripple at the capacitor voltage, f_o is the AC mains frequency, and P is the nominal output power.

If $v_c = 250$ V, $f_o = 60$ Hz, $P = 200$ W, and $\Delta v_c = 1\%$, a value of $C = 266\,\mu$F is obtained. It is approximated to the next highest commercially available value of 330 μF. For practical purposes, an electrolytic type capacitor was selected.

The output inductor can be calculated with

$$L = \frac{V_L D}{\Delta I_L f_s}, \tag{5}$$

where ΔI_L is the desired current ripple at the inductor, f_s is the switching frequency of the inverter, V_L is the voltage at the inductor, and D is the equivalent duty cycle of the inverter.

Considering a worst-case design for the duty cycle, the zero crossing the grid voltage, a duty cycle of $D = 0.5$ was

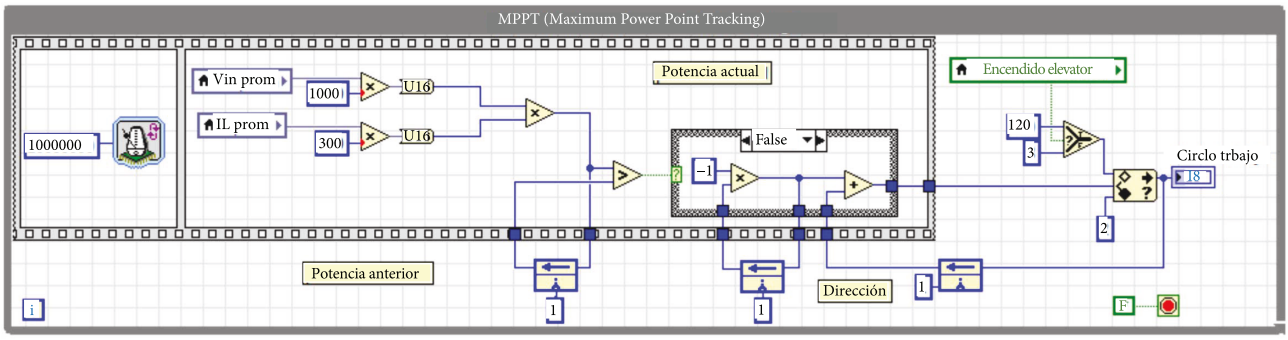

(a)

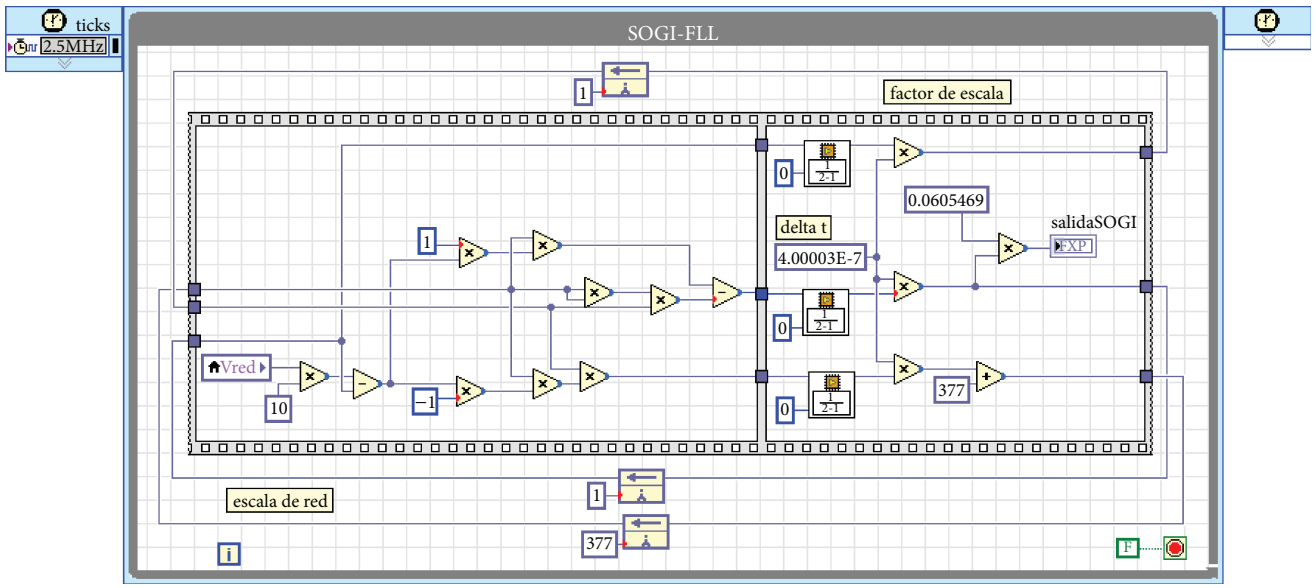

(b)

Figure 4: LabVIEW control blocks implemented on the CompactRIO platform. (a) MPPT algorithm. (b) Synchronization controller.

selected. If $f_s = 90\,\text{kHz}$, $V_L = 250\,\text{V}$, and an allowed current ripple $\Delta I_L = 10\%$, a value of $L = 3.96\,\text{mH}$ is obtained.

The design of the DC/DC boost converter can be calculated as a classical one, so it is not discussed in this paper.

2.2.1. Controller Stage. There are several MPPT algorithms [12–15] reported in the literature that can be used for the DC/DC boost converter. A classic perturb and observe (P&O) method has been used in this work.

For the inverter, a sliding mode control has been considered. It provides advantages like stability at large variations in load and voltage, robustness, good dynamic response, and easy implementation [16].

The sliding mode controller is based on the theory of variable structures [16, 17], so power converters are good candidates for this type of control, since they naturally operate in this way.

The controller design begins with the definition of a sliding surface, toward which the system must be attracted and must remain in it (Figure 2). The sliding surface can be a line or a plane in the generalized form. The conditions of existence and stability of the sliding mode control assure its proper operation [16].

Since the converter is intended to operate as an active power filter in addition to the power injection, the grid current i_s must be sinusoidal and in phase with the voltage source v_s, regardless of the existing nonlinear loads connected at the PCC at the grid. Then, the AC current must be

$$i_s = k v_s, \tag{6}$$

where k determines the actual power demanded by the load plus the energy available at the PV panels.

The proposed sliding surface is

$$\sigma = i_s - k v_s, \tag{7}$$

and the control laws considered are

$$u_1 = \begin{cases} 1, & \text{for } \sigma > 0, \\ 0, & \text{for } \sigma < 0, \end{cases} \qquad u_3 = \begin{cases} 1, & \text{for } v_s < 0, \\ 0, & \text{for } v_s > 0. \end{cases} \tag{8}$$

2.3. Existence of the Sliding Mode. The existence condition ensures that the equation system will be maintained in

Table 1: Simulation and experimental parameters.

Photovoltaic array	
Maximum power	200 W
Open-circuit voltage	92 V
Short-circuit current	4.76 A
Nominal voltage (MPP)	67 V
Nominal current (MPP)	3.6 A
Topology	
DC/DC boost converter inductor L_e	3.5 mH
DC link voltage	250 V
Energy storage capacitor C	330 μF
Output inductor L	4 mH
DC/DC boost converter switching frequency F_s	39 kHz
Inverter switching frequency F_d	90 kHz
PI controller	
Gain	0.05
Time constant	0.05
Nonlinear load	
Power factor	68%
Apparent power	105 VA
Grid	
Frequency	60 Hz
Grid voltage	120 V rms

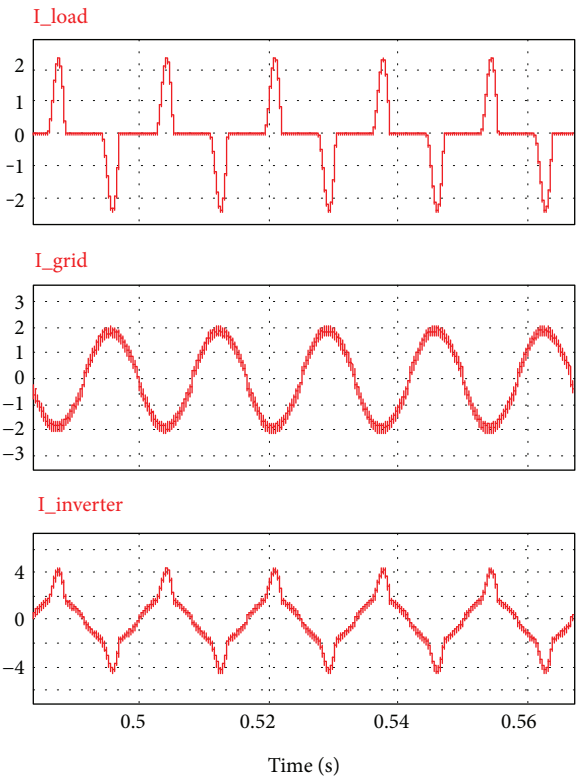

Figure 5: System injecting and alleviating the harmonic distortion. From (a) to (c): load current (1 A/div), grid current (1 A/div), and inverter current (2 A/div).

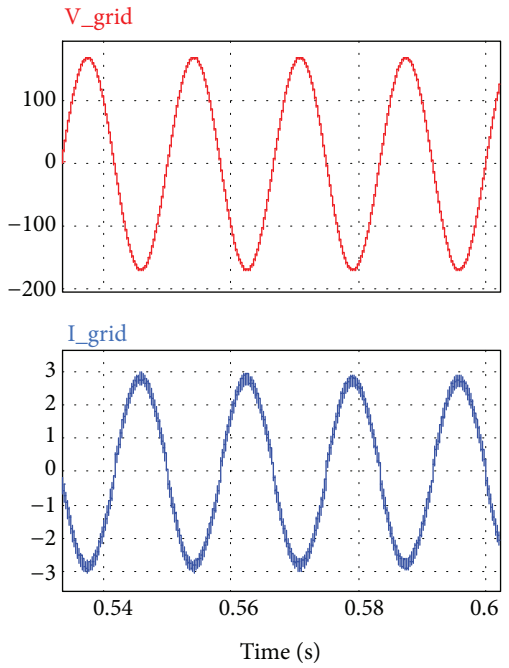

Figure 6: Topology injecting only active power. From (a) to (b): grid voltage (100 V/div) and grid current (1 A/div).

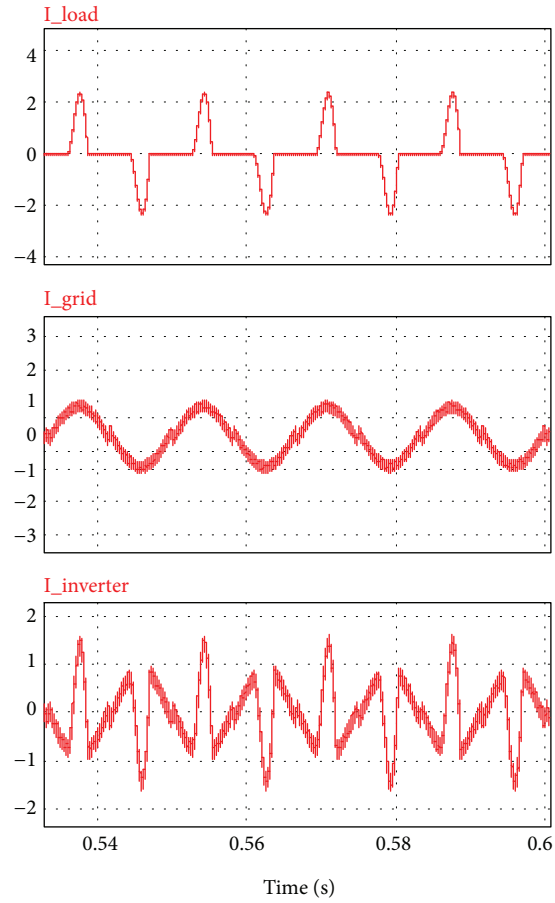

Figure 7: Operation as an active power filter. From (a) to (c): load current (2 A/div), grid current (1 A/div), and inverter current (1 A/div).

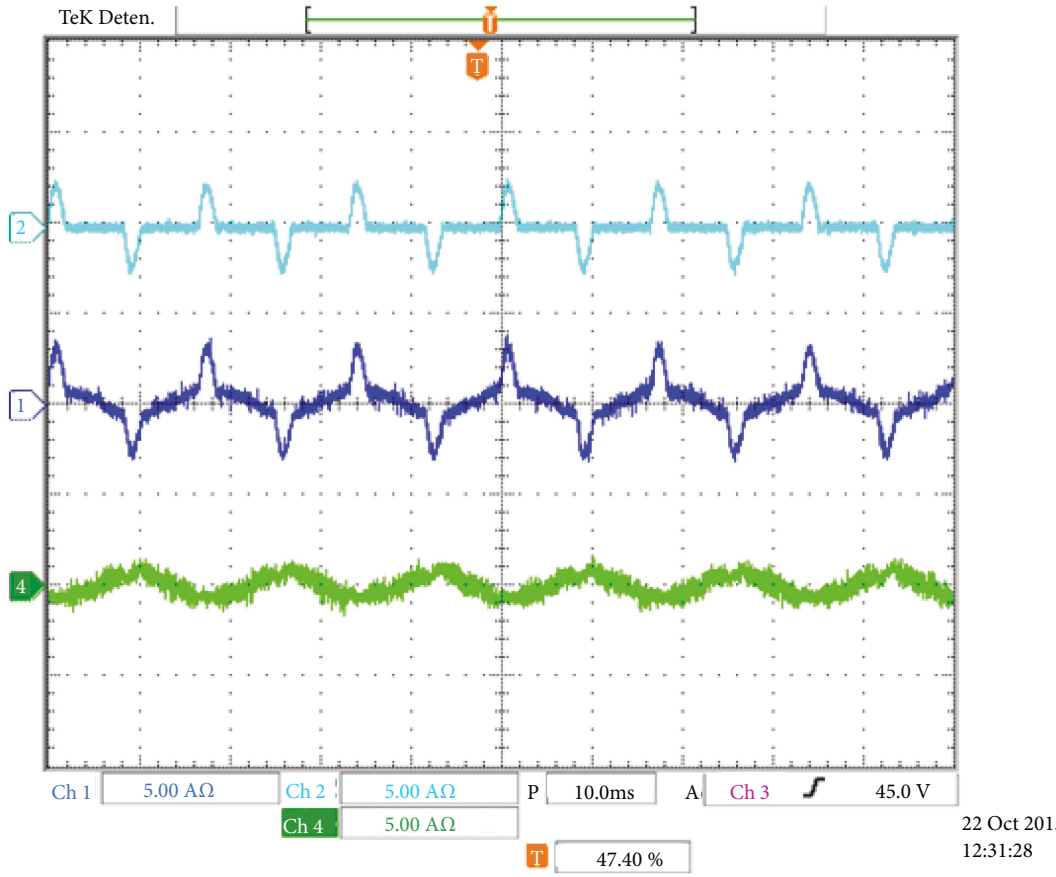

Figure 8: Experimental results for the system injecting and alleviating the harmonic distortion. From top to bottom: load current (5 A/div), inverter current (5 A/div), and grid current (5 A/div).

the sliding surface. It implies satisfying the following inequality [16]:

$$\sigma\sigma' < 0. \tag{9}$$

By deriving (7), (10) is obtained:

$$\sigma' = i_s' - kv_s'. \tag{10}$$

Considering Figure 1 and by applying the first Kirchhoff law at the PCC, (11) is obtained:

$$i_s = i_{\text{load}} - i_L. \tag{11}$$

With the derivative of (11) and by substituting it in (10) together with (1), (12) can be obtained:

$$\sigma' = i_{\text{load}}' - \frac{v_c}{L}(u_1 - u_3) + \frac{v_s}{L} - kv_s'. \tag{12}$$

Considering $v_s = V_P \sin(\omega t)$, using (8) and (9), the existence conditions of the sliding surface are obtained.

If σ and v_s are both positive then, due to the control laws, $u_1 = 1$ and $u_3 = 0$. Therefore,

$$-\frac{v_c}{L} + \frac{V_P \sin(\omega t)}{L} - k\omega V_P \cos(\omega t) < -i_{\text{load}}'. \tag{13}$$

If σ and v_s are both negative then, due to the control laws, $u_1 = 0$ and $u_3 = 1$. Therefore,

$$\frac{v_c}{L} + \frac{V_P \sin(\omega t)}{L} - k\omega V_P \cos(\omega t) > -i_{\text{load}}'. \tag{14}$$

If $\sigma < 0$ and $v_s > 0$, then, due to the control laws, $u_1 = 0$ and $u_3 = 0$. Then,

$$\frac{V_P \sin(\omega t)}{L} - k\omega V_P \sin(\omega t) > -i_{\text{load}}'. \tag{15}$$

If $\sigma < 0$ and $v_s < 0$, then, due to the control laws, $u_1 = 1$ and $u_3 = 1$.

Then,

$$\frac{V_P \sin(\omega t)}{L} - k\omega V_P \sin(\omega t) < -i_{\text{load}}'. \tag{16}$$

To satisfy (13) and (14) inequalities, the selected capacitor voltage v_c should be much higher than the peak of the AC mains V_p. To satisfy (15) and (16) inequalities, the load should be smooth.

The stability analysis is beyond the purpose of this paper, but previous analysis allows assurance of the proper operation of the system in the sliding surface. To determine the stability, an equivalent control method can be employed [17]. An equivalent control has to be found once the system is in

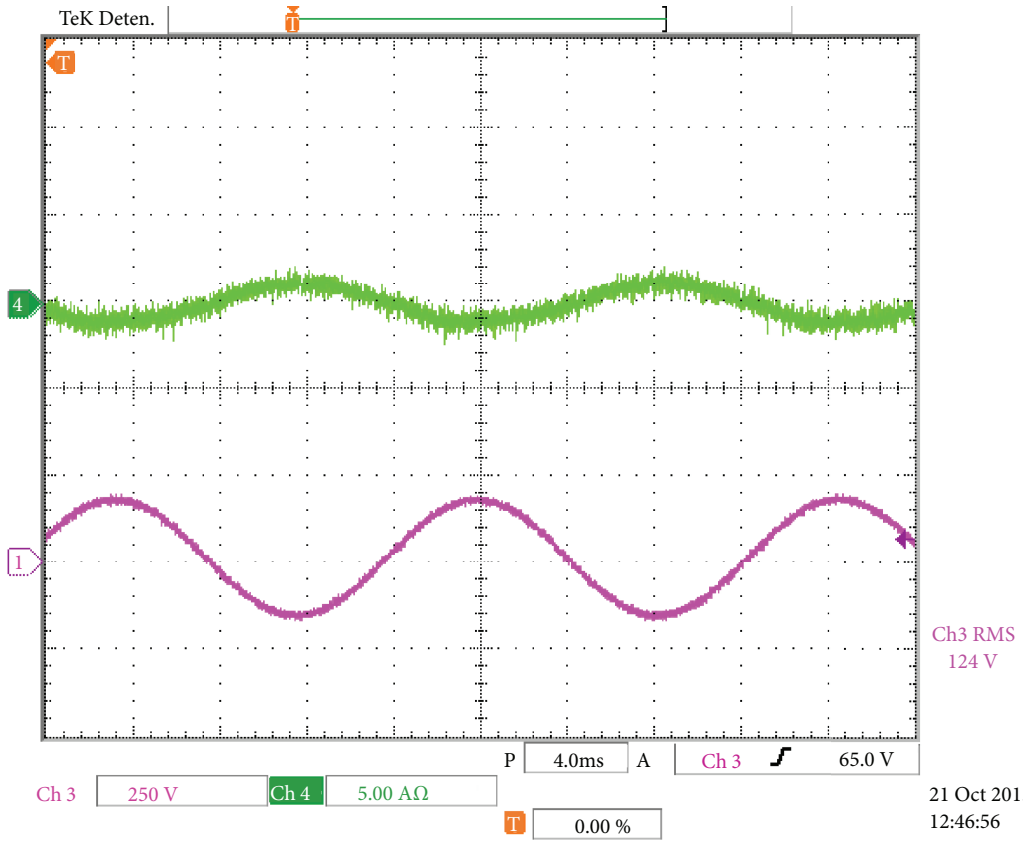

Figure 9: Experimental results when the topology only injects the active power. From top to bottom: grid current (5 A/div) and grid voltage (250 V/div).

the sliding surface, and then, the resultant differential equation system is evaluated for stability. This can be done by means of Lyapunov function [18] or by linearization.

2.4. Other Controller Blocks. For the proper operation of the system, other important control blocks must be taken into account, that is, the MPPT algorithm, the grid synchronization algorithm, and the voltage reference generator to control the capacitor voltage.

The constant k for the control of the capacitor voltage is determined by a PI controller, as in [19, 20]. To ensure a good steady-state operation of the system and thus a high power factor, this controller is tuned for a slow response.

The SOGI-FLL [21] is considered for the synchronization with the grid. This algorithm is capable of generating a good reference under distorted grid conditions.

Finally, other blocks, like blanking time and protections, are considered in the final implementation.

2.4.1. Digital Platform. As mentioned before, the platform considered for the control implementation is the CompactRIO from NI, together with the LabVIEW visual programming software. There have been programmed system protections and controllers for the entire system.

Figure 3 shows the control panel. The user can select several waveforms to be graphed in real time. Also, the FFT can be obtained, by selecting the appropriate tab on the control panel.

In Figure 4, some of the controllers implemented are shown. Specifically, the MPPT algorithm based on the P&O method is shown in Figure 4(a), and the SOGI-FLL controller employed for the synchronization with the grid is shown in Figure 4(b).

As part of the protections, overvoltage and overcurrent detection is included, but the blanking time of the inverter branch is also included in the program.

3. Simulation and Experimental Results

The system shown in Figure 1 was numerically simulated and physically implemented. The PSIM software was selected for simulations because of its ease of use and versatility. It also includes models for the PV panels. For the implementation of the switches, SiC devices were used. Table 1 shows the parameters considered for the system.

The nonlinear load considered is a traditional single-phase full-bridge diode rectifier plus a capacitive filter; the total harmonic distortion of this current is above 100%.

3.1. Simulation Results. The steady-state operation of the proposed system is illustrated in Figure 5. In this test, the load demands a high harmonic current content and the PV panels deliver more power than that absorbed by the load, so energy is injected to the grid. In Figure 5(a), the current demanded by the nonlinear load is shown. In Figure 5(b), the low distorted grid current can be observed; in this case, it should

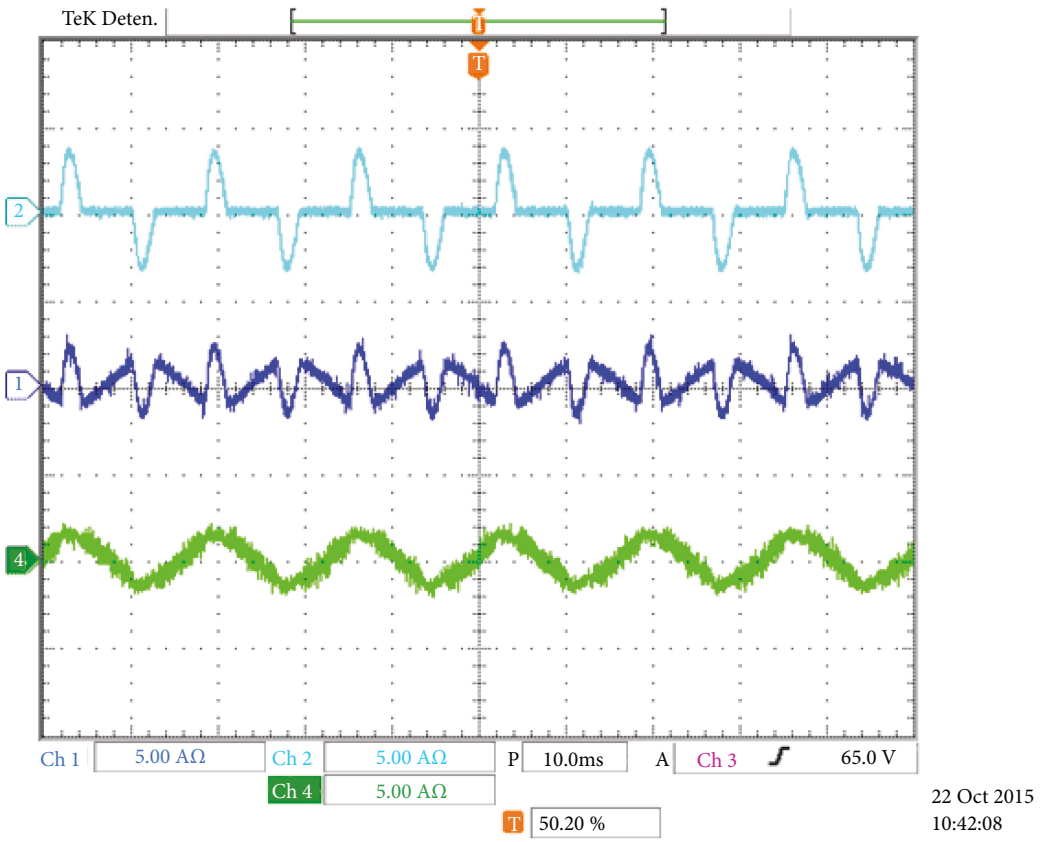

Figure 10: Experimental results when the converter operates only as an active filter. From top to bottom: load current (5 A/div), inverter current (5 A/div), and grid current (5 A/div).

be noted that this current is 180 degrees out of phase with the load current. In Figure 5(c), the inverter current is shown, where it can be observed that it is injecting both active power and harmonic currents. The power factor at the PCC is 0.99.

The operation of the system without nonlinear load is shown in Figure 6. In this case, the converter operates as a traditional grid-connected PV system. Only active power is injected into the grid. The current is 180 degrees out of phase with the grid voltage.

Additionally, the proposed system has the advantage of operating as a conventional active filter, as shown in Figure 7. In this case, the power from the PV panels is null. In Figure 7(a), the distorted load current can be observed. In Figure 7(b), the low distorted grid current is shown, which is in phase with the grid voltage. In Figure 7(c), the compensating current from the inverter can be observed.

3.2. Experimental Results. The steady-state operation of the proposed system is shown in Figure 8. In this test, the load demands a high harmonic current content and the PV panels provide more power than that absorbed by the nonlinear load, so energy is injected to the grid. At the top of the figure, the high distorted current demanded by the nonlinear load is shown (THD = 164%). At the bottom of the figure, the low distorted grid current can be observed (THD = 4.34%). Note that this current is 180 degrees out of phase with the nonlinear load current, as expected. At the center of the figure, the inverter current is shown, where it can be observed that it is injecting both active power and harmonic current components. The power factor at the PCC is 0.99.

The operation of the system without load is shown in Figure 9. In this case, the converter operates as a traditional grid-connected PV system. Only active power is injected into the grid. The current is 180 degrees out of phase with the grid voltage.

Additionally, the proposed system has the advantage of operating as a conventional active filter, as shown in Figure 10. In this case, the power from the PV panels is null. At the top of the figure, the distorted load current can be observed. At the bottom of the figure, the grid current is shown, which is in phase with the grid voltage. At the center of the figure, the compensating current of the inverter can be observed.

4. Conclusion

Grid-connected PV systems usually inject active power energy to the grid. They are mainly used to avoid the dependence of fossil fuels. Since the power stage used in grid-connected applications is an inverter, the functionality of this stage may be increased, acting as an active power filter and a power factor corrector.

In this paper, a multifunctional grid-connected PV system is analyzed and tested. The power stage consists of a

DC/DC boost converter and a single-phase inverter. The converter's protections and controllers are implemented in the CompactRIO digital platform from NI, which allows user friendly and easy tuning of the system. A sliding mode controller is employed that permits good operation in different modes: when the system delivers energy and compensates harmonics, when it only injects energy, or when it only acts as an active power filter.

The operation, design, and implementation of the system are presented. The simulation and experimental results confirm the feasibility of the proposal.

Conflicts of Interest

The authors declare that there is no conflict of interest regarding the publication of this paper.

Acknowledgments

This work has been sponsored by National Instruments Corporation through the 2016 NI Academic Research grant program and also was supported in part by the Comunidad de Madrid government (SINFOTON-CM) (S2013/MIT-2790).

References

[1] Renewable Energy Policy Network for the 21st Century, *Global Status Report 2014*, 2014, http://www.ren21.net/ren21activities/globalstatusreport.aspx.

[2] V. E. Wagner, J. C. Balda, D. C. Griffith et al., "Effects of harmonics on equipment," *IEEE Transactions on Power Delivery*, vol. 8, no. 2, pp. 672–680, 1993.

[3] N. R. Raju, S. S. Venkata, R. A. Kagalwala, and V. V. Sastry, "An active power quality conditioner for reactive power and harmonics compensation," in *1995 PESC '95 Record, 26th Annual IEEE Power Electronics Specialists Conference*, vol. 1, pp. 209–214, Atlanta, GA, USA, June 1995.

[4] A. M. Massoud, S. J. Finney, and B. W. Williams, "Seven-level shunt active power filter," in *2004 11th International Conference on Harmonics and Quality of Power*, pp. 136–141, Lake Placid, NY, USA, September 2004.

[5] S. Inoue, T. Shimizu, and K. Wada, "Control methods and compensation characteristics of a series active filter for a neutral conductor," *IEEE Transactions on Industrial Electronics*, vol. 54, no. 1, pp. 433–440, 2007.

[6] J. He, Y. Wei Li, F. Blaabjerg, and X. Wang, "Active harmonic filtering using current-controlled, grid-connected dg units with closed-loop power control," *IEEE Transactions on Power Electronics*, vol. 29, no. 2, pp. 642–653, 2014.

[7] P. C. Tan, Z. Salam, and A. Jusoh, "A single-phase hybrid active power filter using extension p-q theorem for photovoltaic application," in *2005 International Conference on Power Electronics and Drives Systems*, vol. 2, pp. 1250–1255, Kuala Lumpur, Malaysia, 2005.

[8] P. Neves, D. Goncalves, J. G. Pinto, R. Alves, and J. L. Afonso, "Single-phase shunt active filter interfacing renewable energy sources with the power grid," in *2009 35th Annual Conference of IEEE Industrial Electronics*, pp. 3264–3269, Porto, Portugal, November 2009.

[9] S. A. O. da Silva, L. P. Sampaio, and L. B. G. Campanhol, "Single-phase grid-tied photovoltaic system with boost converter and active filtering," in *2014 IEEE 23rd International Symposium on Industrial Electronics (ISIE)*, pp. 2502–2507, Istanbul, Turkey, June 2014.

[10] I. Méndez, N. Vázquez, J. Vaquero, J. Vázquez, C. Hernández, and H. López, "Multifunctional grid-connected photovoltaic-system controlled by sliding mode," in *IECON 2015 - 41st Annual Conference of the IEEE Industrial Electronics Society*, pp. 1339–1344, Yokohama, Japan, November 2015.

[11] M. C. Di Piazza and G. Vitale, "Static model," in *Photovoltaic Sources Modeling and Emulation*, pp. 56–67, Springer-Verlag, London, 2013.

[12] S. K. Dash, D. Verma, S. Nema, and R. K. Nema, "Comparative analysis of maximum power point (MPP) tracking techniques for solar PV application using MATLAB simulink," in *2014 Recent Advances and Innovations in Engineering (ICRAIE)*, pp. 1–7, Jaipur, India, May 2014.

[13] A. Morales-Acevedo, J. L. Diaz-Bernabe, and R. Garrido-Moctezuma, "Improved MPPT adaptive incremental conductance algorithm," in *IECON 2014 - 40th Annual Conference of the IEEE Industrial Electronics Society*, pp. 5540–5545, Dallas, TX, USA, October–November 2014.

[14] R. B. Roy, E. Basher, R. Yasmin, and M. Rokonuzzaman, "Fuzzy logic based MPPT approach in a grid connected photovoltaic system," in *2014 8th International Conference on Software, Knowledge, Information Management and Applications (SKIMA)*, pp. 1–6, Dhaka, Bangladesh, December 2014.

[15] N. Vázquez, Y. Azaf, I. Cervantes, E. Vázquez, and C. Hernández, "Maximum power point tracking based on sliding mode control," *International Journal of Photoenergy*, vol. 2015, Article ID 380684, 8 pages, 2015.

[16] A. A. Agrachev, A. S. Morse, E. D. Sontag et al., *Nonlinear and Optimal Control Theory*, Springer, Italy, 2004.

[17] J. Y. Hung, W. Gao, and J. C. Hung, "Variable structure control: a survey," *IEEE Transactions on Industrial Electronics*, vol. 40, no. 1, pp. 2–22, 1993.

[18] R. Sepulchre, M. Jankovic, and P. V. Kokotovic, *Constructive Nonlinear Control*, Springer Verlag, London, 1997.

[19] D. A. Torrey and A. M. A. M. Al-Zamel, "Single-phase active power filters for multiple nonlinear loads," *IEEE Transactions on Power Electronics*, vol. 10, no. 3, pp. 263–272, 1995.

[20] J. Matas, L. G. de Vicuna, J. Miret, J. M. Guerrero, and M. Castilla, "Feedback linearization of a single-phase active power filter via sliding mode control," *IEEE Transactions on Power Electronics*, vol. 23, no. 1, pp. 116–125, 2008.

[21] R. Villalobos Mendoza, *Design and Implementation of a Digital Circuit for Phase Synchronization of Applications with Interconnection with the Grid, (in Spanish), [M.S. thesis]*, Instituto Tecnológico de Celaya, Gto, Mexico, 2013.